Dopant Mapping of Semiconductors with Scanning Electron Microscopy

Daisuke TSURUMI* and Kotaro HAMADA

This paper investigates the decrease in dopant contrast of semiconductors due to the surface contamination caused by electron irradiation during scanning electron microscopy (SEM) observation. We have revealed that secondary electron (SE) high-pass energy filtering can significantly reduce the influence of contamination, and thus the dopant contrast remains stable during observation. In addition, the contrast is observable even at high magnification by simultaneous application of the SE energy filtering and a reverse bias voltage because the reverse bias voltage increases the contrast and relatively decreases the sensitivity to the contamination. These imaging techniques enable accurate and reproducible dopant mapping that cannot be achieved with conventional SE imaging techniques, and are therefore expected to be a significant contribution to the semiconductor manufacturing industry.

Keywords: dopant mapping, high-pass energy-filtered imaging, SEM, contamination, InP

1. Introduction

Compound semiconductor devices, as typified by laser diodes, photo diodes, and high electron mobility transistors, are used for optical communication systems, satellite communications, and cellular base stations to meet a growing demand for large-capacity and high-speed communication systems that play a key role in the infrastructure of modern society. The properties and reliability of semiconductor devices are thus becoming increasingly important. Therefore, in addition to electrical evaluation, physical analysis to observe the configuration and composition of these devices is required in order to improve device performance. Physical analysis also provides important information on the electrically active dopant distribution and concentration, which determine the properties of semiconductor devices and therefore require precise control.

Therefore, a large number of dopant profiling techniques have been developed. One of the most attractive techniques that can meet industrial demands for rapid data measurement and quick sample preparation is a scanning electron microscopy (SEM).

Dopant contrast observation using SEM was hardly reported until the 1990s; however, substantial progress was made with this technique after Perovic et al. demonstrated that the contrast of the observed SE intensity was not only dependent on the type of doping, but was also sensitive to the doping concentration levels[1]. In 1998, a linear dependence was reported between the observed contrast and the logarithm of the dopant concentration in *p*-type Si[2]. This was confirmed for dopant concentrations in the range from 10^{16} to 10^{20} cm^{-3}[3]. In 2006, it was demonstrated that dopant contrast could be observed from even focused ion beam (FIB)-prepared silicon *p*-*n* junctions[4].

Thus, dopant contrast observation using SEM is a very important method for the process development and failure analysis of semiconductor devices because it is a quick and highly sensitive technique. However, there are problems to be overcome, such as the reported reversal of contrast with different primary beam energy from Si with a thick oxide layer[5]. A decrease in contrast is also observed during SEM observation, which causes surface contamination*1[6]. It was revealed that SEM was sensitive to the dopant concentration in the *p*-type region, but not to that in the *n*-type region[7]. In addition, the interpretation of III-V semiconductor devices at the interface of heterostructures is more complicated than that for silicon homostructures[8], and accordingly it is difficult to observe accurate dopant distributions.

Therefore, we have focused on solving such problems to achieve accurate dopant mapping. In this paper, we report the decrease in contrast due to contamination and propose methods to solve the problem.

2. Experiments

2-1 Mechanism of dopant contrast in SEM

The contrast in SEM images can be categorized as topographic, material, voltage, channeling contrast, etc. The mechanism of the dopant contrast isn't completely understood yet. One popular model is that the contrast is caused by local external electric fields above the sample surface, called patch field, due to the carrier concentration[9]. In order to explain this theory, **Fig. 1** shows a schematic drawing of the potential distribution for a *p*-*n* junction in an SEM chamber and the SEM image obtained. The inherent potential of a *p*-*n* junction leads to an external electric field in the vacuum region above the sample surface. The electric field is positive above the *n*-type region and negative above the *p*-type region. Hence the secondary electrons (SEs) above the *n*-region experience acceleration toward the specimen by electrostatic force, whereas those above the *p*-region are accelerated away from the specimen, as shown in **Fig. 1 (a)**. As a result, the collection efficiency of the SEs from the *p*-type region increases and that from the *n*-type region decreases, so that a brighter *p*-type contrast and darker *n*-type contrast are observed across the *p*-*n* junction in the SEM micrograph shown in **Fig. 1 (b)**.

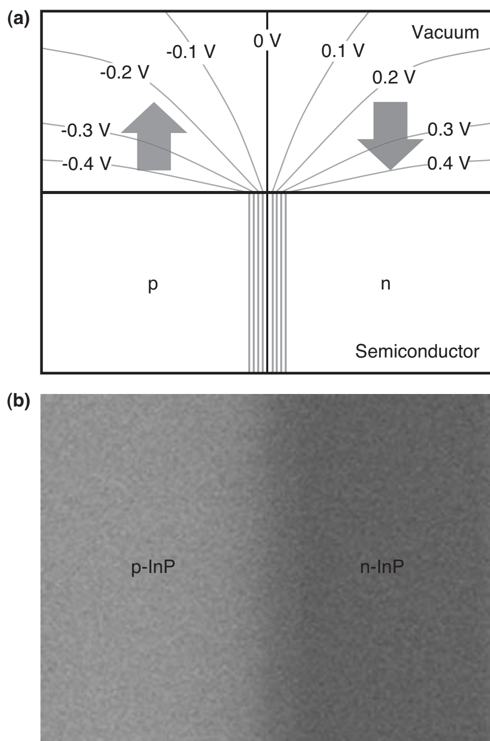

Fig. 1. (a) Schematic diagram of potential distribution inside and outside a specimen with a symmetric *p-n* junction, (b) SEM image of the *p-n* junction

2-2 Experimental method

SEM images were collected using a through-the-lens detector in a Hitachi S-4800 FE-SEM. The detector system has a control electrode that enables the generation of high-pass energy-filtered images. **Figure 2** shows a schematic drawing of the detection system with the SE high-pass energy-filtering method that shows the behavior of the SEs and back scattered electrons (BSEs).

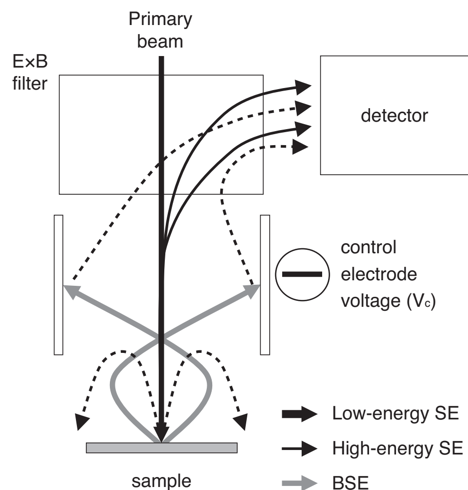

Fig. 2. Schematic drawing of SE high-pass energy filtering in a Hitachi S-4800 microscope with a through-the-lens detector

The SEM is equipped with a snorkel objective lens*2 that produces a strong magnetic field above the SEM specimen, which causes the SEs from the sample to move up to the detector. A negative voltage (V_c) is applied to the control electrode, which generates a negative electric field. The SEs with energy less than V_c cannot pass through the electric field. By changing V_c, the minimum energy of the SEs that are collected by the detector can be selected, thus generating high-pass energy-filtered images.

At V_c = 0 V, no negative electric field exists, so that almost all the SEs can reach the detector, which results in unfiltered images.

In contrast, the BSEs pass through the negative electric field due to their high energy. These electrons generated at low angles collide with the control electrode, where they are converted into SEs. These SEs retain the contrast information of the original BSEs and are collected by the detector. However, the number of BSEs is generally much smaller than the number of SEs; therefore, the images mainly contain information related to the SEs.

2-3 Evaluation method and specimen

An indium phosphide (InP) test structure was grown by chemical vapor deposition that consisted of a *p*-type layer (1×10^{18} Zn atoms cm^{-3}) on an *n*-type substrate (1×10^{18} Sn atoms cm^{-3}). The sample was cleaved in air prior to loading into the SEM chamber. The images were taken using an accelerating voltage of 1.0 kV and a working distance of 2.0 mm. The intensities of the *p*- and *n*-type layers in the SEM images were extracted from 256 gray level*3 images.

3. Results and Discussion

3-1 Reduction of decreased contrast during observation

When a sample surface is observed using SEM, it is strongly affected by the surface condition. In particular, contamination generated during SEM observation is a major issue. Repeated observation of the same area increases the influence of contamination and decreases the dopant contrast. Thus, it is difficult to obtain accurate dopant mapping. To solve this problem, it is necessary to reduce the influence of contamination.

The commonly known solutions are to decrease the irradiated electron beam current for SEM observation, using a cold trap, and to increase or decrease the specimen temperature(10). However, the effects of these methods are often insufficient. Therefore, we attempted to remove the influence of contamination using SE energy filtering(11).

(1) Influence of contamination

To investigate the main factor that causes the decrease in contrast by contamination, SE energy distributions of surfaces cleaved and covered with contamination were observed. SE energy distributions were obtained using SEM intensities as a function of V_c. The observed intensities of the surfaces from the *p*- and *n*-type regions represent the total number of electrons with energy higher than the cutoff energy V_c. Therefore, experimental SE distributions were obtained by differentiating the total signal intensity with respect to V_c.

Figure 3 (a) shows the intensity profiles from the *p*-type and *n*-type regions of SEM images as a function of V_c for freshly cleaved surfaces and those covered with the contamination layer. A contamination layer was intentionally formed on the cleaved *p*-*n* regions by irradiation during SEM observation. The same contrast and brightness settings were used for all images.

Figure 3 (b) shows the SE energy distribution obtained by differentiating the total signal intensity with respect to V_c shown in **Fig. 3 (a)**. The results indicate that the total SE emission yield decreases after the irradiation. In addition, the contrast (intensity difference) between the *p*- and *n*-type regions is obtained especially in the range of $3 V \leq V_c \leq 6 V$.

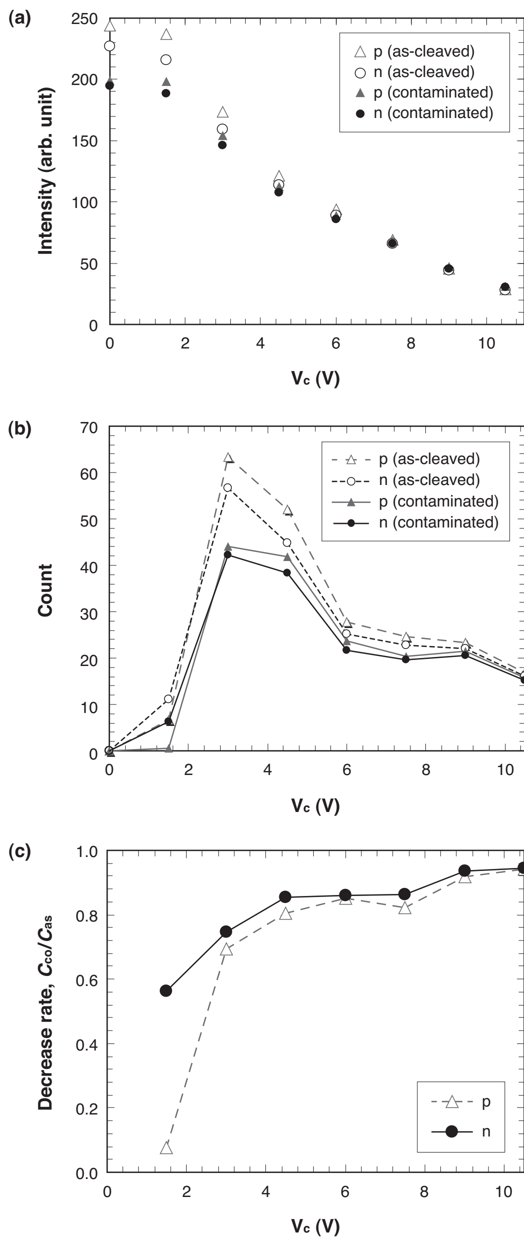

Fig. 3. (a) SE intensity as a function of V_c, (b) Experimental SE distributions, (c) SE energy dependence of the decrease rate (counts) due to irradiation during SEM observation

Figure 3 (c) shows the dependence of the decrease rate (C_{co}/C_{as}) on the SE energy due to the SEM observation, where C_{co} and C_{as} are the counts of experimental SE distributions (**Fig. 3 (b)**) from the contamination and as-cleaved surfaces, respectively.

Figure 3 (c) shows the lower energy SE emissions, especially in the range from $V_c = 0$ to 3 V of the *p*-type region, decreased by *ca.* 90% after the SEM observation, while those of the *n*-type region decreased by *ca.* 30%. In contrast, the SE emissions that caused dopant contrast (in the range from $V_c = 3$ to 6 V) were decreased by *ca.* 20% in both the *p*- and *n*-type regions. Therefore, a higher SE energy results in a weaker influence of the contamination caused during SEM observation.

These results indicate that through the use of SE energy filtering, which does not collect low-energy SEs that are strongly affected by contamination, it is possible to reduce the influence of contamination and the dopant contrast is expected to remain stable during SEM observation. Therefore, the effect of SE energy filtering was further investigated.

(2) Results of SE energy filtering

Figure 4 shows unfiltered ($V_c = 0$ V) and filtered ($V_c = 3$ V) SE images of a *p*-*n* junction at 20,000× magnification. To investigate the effect of filtering, dopant contrast was observed as a function of SEM observation time, *t*. The contrast and brightness settings in each detection mode were adjusted so that the contrast was clearly observed at t = 1 s, and images at t = 1 to 80 s were acquired at the same settings.

Figure 4 shows that the dopant contrast after 1 s of SEM observation was clearly observable in both detection modes. However, in the unfiltered image, the contrast decreased with increasing observation time. Finally, after 80 s, no contrast was observed. This decrease in contrast is caused by the contamination that occurs during SEM observation.

The contrast of the filtered images remained stable during continuous SEM observation and was clearly observable, even after 80 s. This is because filtering removes the influence of contamination, so that the signal of dopant contrast can be clearly detected.

Thus, filtered imaging can reduce the decrease in dopant contrast due to the SEM observation because this method removes low-energy SEs that are strongly affected by surface contamination.

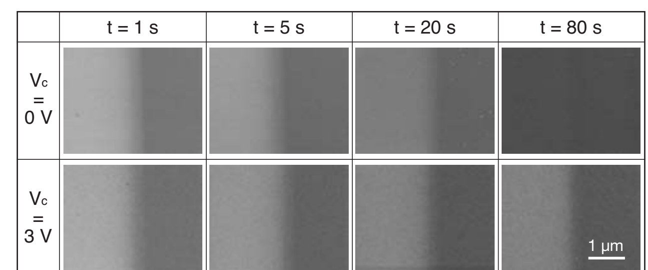

Fig. 4. Unfiltered and filtered SE images of a *p*-*n* junction after SEM observation

3-2 Reduction of decreased contrast at high magnification

SE energy filtering has been demonstrated as effective to reduce the decrease in contrast during continuous SEM observation. However, the SE contrast deteriorates with increased magnification, even for SE energy-filtered images. This is because the irradiation dose per unit area increases at high magnification, which leads to a significant influence of contamination.

Then, the effect of reverse bias voltage (V_r) application was investigated. The resulting the contrast was clearly observed at magnifications as high as 250,000× by simultaneously applying SE energy filtering and a reverse bias voltage[12].

(1) Effect of reverse bias voltage application

A reverse bias voltage was applied across the *p*-*n* junction of InP in situ during SEM observation, as schematically shown in **Fig. 5**.

To investigate the effect of V_r, SE intensities from the *p*- and *n*-type regions were obtained using an unfiltered imaging method. The same contrast and brightness settings were used for all measurements.

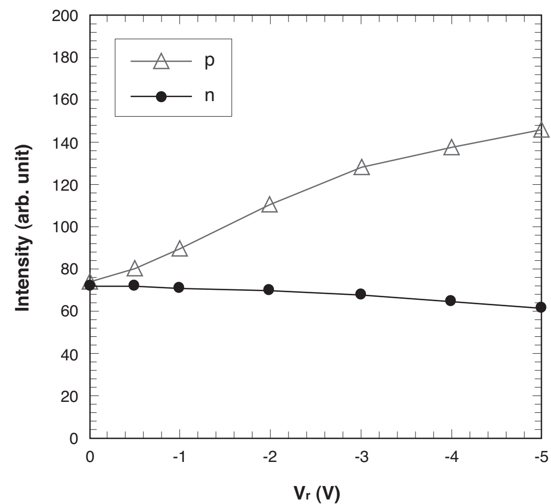

Fig. 6. SE intensities of both *p*- and *n*-type layers as a function of the reverse bias voltage

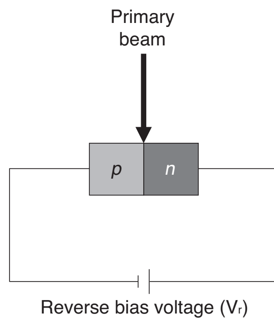

Fig. 5. Schematic diagram of reverse bias voltage application

	×10,000	×50,000	×250,000
(a) V_r = 0 V V_c = 0 V	2 μm	500 nm	100 nm
(b) V_r = -3 V V_c = 0 V			
(c) V_r = 0 V V_c = 3 V			
(d) V_r = -3 V V_c = 6 V			

Fig. 7. SEM images obtained using various detection modes: (a) unfiltered without reverse bias voltage, (b) unfiltered with reverse bias voltage, (c) filtered without reverse bias voltage, and (d) filtered with reverse bias voltage

Figure 6 shows the SE intensities as a function of V_r. The contrast increased with increased reverse biasing of the junction because the reverse bias voltage increases the potential barrier, as reported in ref.[4]. When the contrast is increased by application of a reverse bias voltage, there is a relative decrease in the influence by contamination. Therefore, this method was applied to high-magnification SEM observation of a *p*-*n* junction.

(2) Results of reverse bias voltage application

SEM images of the *p*-*n* junction in InP, as shown in **Fig. 7**, were obtained at magnifications ranging from 10,000× to 250,000×. The detection modes employed to obtain images were (a) unfiltered without reverse bias voltage, (b) unfiltered with reverse bias voltage, (c) filtered without reverse bias voltage, and (d) filtered with reverse bias voltage.

At 10,000× magnification, the contrast and brightness settings were adjusted to achieve visible dopant contrast in all detection modes. The images at magnification from 10,000 to 250,000× were then acquired at the same settings.

The contrast of the *p*-*n* junction was clearly observed using detection mode (d), even at 250,000× magnification, while it decreased with increasing magnification for detection modes (a) to (c) and no contrast was observed at 250,000× magnification.

Figure 8 shows the intensity profiles as a function of magnification. For detection mode (a), the intensities from the *p*- and *n*-type layers rapidly decreased with increasing magnification.

For detection mode (b), the intensities from the *n*-type layer decreased slightly because application of the reverse bias voltage reduces the influence of contamination. However, the intensity from the *p*-type layer decreased to almost the same intensity level as that from the *n*-type layer,

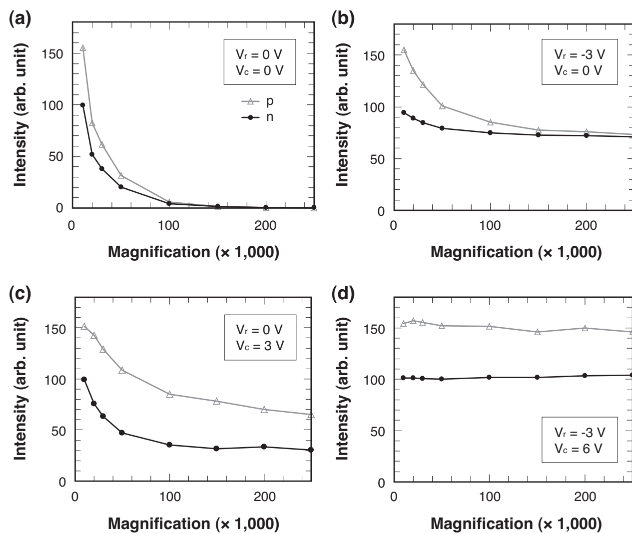

Fig. 8. Intensity profiles for each detection mode as a function of magnification

and therefore the dopant contrast could not be observed at 250,000× magnification.

For detection mode (c), the intensity difference between the *p*- and *n*-type regions was retained, even at high magnification. However, the intensities decreased with increasing magnification, and very little dopant contrast was observed at 250,000× magnification. This indicates that high-energy SEs are also affected by the contamination during high-magnification observation.

For detection mode (d), the intensities from both the *p*- and *n*-type layers remained constant at magnifications ranging from 10,000× to 250000×, due to the effects of both the SE energy filtering and reverse bias voltage. Therefore, the contrast could be clearly observed, even in the image obtained at 250,000× magnification.

Thus, when both energy filtering and reverse bias voltage are employed, the influence of contamination can be substantially reduced and contrast can be observed at high magnification.

4. Conclusion

This work highlights the problem of decreased dopant contrast due to contamination caused by electron irradiation during SEM observation. The SE energy distribution indicates that contamination causes a decrease of low-energy SE emissions, which reduces the contrast in unfiltered SE images. The unfavorable influence of contamination can be substantially reduced with high-pass energy-filtered imaging, and stable contrast can be achieved during continuous SEM observation. In addition, the contrast can be clearly observed even under high-magnification conditions, where the influence of contamination is typically increased, by simultaneously applying SE energy filtering and a reverse bias voltage.

These imaging methods can be widely employed for semiconductor devices to provide accurate and reproducible dopant mapping with a high data acquisition rate and rapid sample preparation, and are therefore expected to be a significant contribution to the semiconductor manufacturing industry.

Technical Terms

*1 contamination: Contaminants deposited on the sample surface. Hydrocarbon gas molecules on the sample are polymerized by electron beam irradiation and deposit on the specimen surface.

*2 Snorkel objective lens: A type of objective lens for high-resolution SEM. The magnetic field is allowed to leak around the specimen by the objective lens design, which results in a reduction of the aberration.

*3 256 gray level: The steps of noticeable difference in contrast used for computing. The intensity of the SEM image contrast was evaluated using 256 steps.

References

(1) D. D. Perovic, M. R. Castell, A. Howie, C. Lavoie, T. Tiedje, and J. S. W. Cole, "Field-Emission SEM imaging of compositional and doping layer semiconductor superlattices," Ultramicroscopy 58, pp.104-113 (1995)
(2) D. Venables, H. Jain, and D. C. Collins, "Secondary electron imaging as a two-dimensional dopant profiling technique: review and update," J. Vac. Sci. Technol. B 16, pp.362-366 (1998)
(3) S. L. Elliott, R. F. Broom, and C. J. Humphreys, "Dopant profiling with the scanning electron microscope-A study of Si," J. Appl. Phys. 91, pp.9116-9122 (2002)
(4) P. Kazemian, A. C. Twitchett, C. J. Humphreys, and C. Rodenburg, "Site-specific dopant profiling in a scanning electron microscope using focused ion beam prepared specimens," Appl. Phys. Lett. 88, pp.212110-1-3 (2006)
(5) C. G. H.Walker, F. Zaggout, and M. M. El-Gomati "The role of oxygen in secondary electron contrast in doped semiconductors using low voltage scanning electron microscopy." J. Appl. Phys. 104, pp. 123713-1-6 (2008)
(6) P. Kazemian, C. Rodenburg, and C. J. Humphreys, "Effect of experimental parameters on doping contrast of Si pn junctions in a FEG-SEM," Microelectron. Eng. 73-74, pp.948-953 (2004)
(7) D. Tsurumi, K. Hamada, and Y. Kawasaki, "Observation of two-dimensional *p*-type dopant diffusion across a p^+-InPn^-–InGaAs interface using scanning electron microscopy," J. Appl. Phys. 113, pp.144901-1-4 (2013)
(8) B. Kaestner, C. Schönjahn, and C. J. Humphreys, "Mapping the potential within a nanoscale undoped GaAs region using a scanning electron microscope," Appl. Phys. Lett. 84, pp.2109-2111 (2004)
(9) A. K. W. Chee, R. F. Broom, C. J. Humphreys, and E. G. T. Bosch, "A quantitative model for doping contrast in the scanning electron microscope using calculated potential distributions and Monte Carlo simulations," J. Appl. Phys. 109, pp.013109-1 -9 (2011)
(10) L. Reimer: Image Formation in Low-Voltage Scanning Electron Microscopy, pp.85-86 SPIE Press, Bellingham, WA, (1993)

(11) D. Tsurumi, K. Hamada, and Y. Kawasaki, "Highly Reproducible Secondary Electron Imaging under Electron Irradiation Using High-Pass Energy Filtering in Low-Voltage Scanning Electron Microscopy," Microsc. Microanal. 18, pp.385-389 (2012)
(12) D. Tsurumi, K. Hamada, and Y. Kawasaki, "Energy-Filtered Secondary-Electron Imaging for Nanoscale Dopant Mapping by Applying a Reverse Bias Voltage," Jpn. J. Appl. Phys. 51, pp. 106503-1-4 (2012)

Contributors (The lead author is indicated by an asterisk (*).)

D. TSURUMI*
• Analysis Technology Research Center

K. HAMADA
• Manager, Analysis Technology Research Center